Eur. Phys. J. A (2019) **55**: 119
DOI 10.1140/epja/i2019-12804-5

THE EUROPEAN PHYSICAL JOURNAL A

Regular Article – Theoretical Physics

Study of the surface energy coefficient used in nuclear proximity potential of the α-nuclei systems from density-dependent nucleon-nucleon interactions

R. Gharaei[a] and S. Mohammadi

Department of Physics, Sciences Faculty, Hakim Sabzevari University, P. O. Box 397, Sabzevar, Iran

Received: 16 May 2019 / Revised: 13 June 2019
Published online: 25 July 2019
© Società Italiana di Fisica / Springer-Verlag GmbH Germany, part of Springer Nature, 2019
Communicated by P. Capel

Abstract. An attempt has been made to study systematically the nuclear surface tension coefficient, γ, of the proximity formalism by using the microscopic double-folding (DF) model with the realistic density-dependent (DD) nucleon-nucleon interaction for the ground-state–to–ground-state α-decays of 235 parent nuclei with $Z = 61$–99. In the calculations of DF model, the nucleon-nucleon (NN) interactions are formulated using the effective M3Y force of the CDM3Y6 based on the G-matrix elements of the Paris interaction. We present a new dependence of the surface energy coefficient γ on the asymmetry parameter A_s of the α-nuclei systems by fitting all of the calculated values. Using the presently obtained formula of the coefficient γ in the proximity potential we calculate the theoretical values of the alpha-decay half-lives for different nuclei in the framework of the Wentzel-Kramers-Brillouin (WKB) approximation. Results of our calculations are compared to the values of the experimental data and proximity potential 1977. Good agreements are found. The quality of the proximity potential accompanied by the analytical formula of the surface energy coefficient is tested for fusion reactions between α-particles and heavy nuclei ^{40}Ca, ^{48}Ti, ^{51}V, ^{59}Co, ^{63}Cu, ^{93}Nb, ^{154}Sm and ^{162}Dy The evaluated α-capture cross sections agreed well with the corresponding experimental data. In the present study, the role of the proton and neutron magic numbers of daughter nuclei and also the Geiger-Nuttall plots of $\log_{10}(T_{1/2})$ *versus* $Q_\alpha^{-1/2}$ for various isotopes of heavy parent nuclei have been studied.

1 Introduction

Alpha emission from a nucleus is a fundamental decay process in which the α-particle formed inside the nucleus tunnels out through the potential barrier. There is no doubt that during recent decades the study of α-decay has always been one of the widely discussed topics of nuclear physics. Nowadays, the radioactive emission of an alpha-particle is recognized as one of the most important channels for decay of the unstable heavy and super-heavy nuclei which can provide some reliable knowledge on nuclear structure and nuclear interactions [1–4]. Moreover, it can be considered as a probe for identifying new isotopes via the observation of a very stable nucleus of ^{4}He from unknown parent nucleus with (A, Z) to a known nuclide with $(A-4, Z-2)$ [5,6]. The first experimental observations of alpha-decay process has been established by Rutherford from the electrical conductivity of uranium [7–9]. Recent experiments on α-decay provide precision data of Q_α values and decay half-lives for a vast range of α-daughter nucleus systems [10–20]. From the theoretical point of view, the formation of an alpha-daughter nucleus system was first explained successfully as a typical effect of quantum tunneling phenomenon by Gamow [21] and independently by Condon and Guerney [22,23] in 1928. Under these conditions, one can expect that the selection of an appropriate model to determine the interacting potential between α-particle and daughter nucleus plays an important role in calculating the alpha-decay half-lives. So far, many effective theoretical approaches have been proposed to calculate the nuclear potential during the alpha-decay process such as the generalized liquid-drop model [24,25], the density-dependent (DD) M3Y double-folding (DF) model [4,26], and the Skyrme-Hartree-Fock mean-field model [19].

The nuclear proximity potential provides a simple and practical formalism to estimate the strength of the nuclear interactions of alpha-daughter systems. On the basis of the "proximity force theorem" [27], when two surfaces are approaching each other, approximately at a distance of 2–3 fm, an additional force due to the proximity of surfaces will appear which is called proximity potential. In

[a] e-mail: r.gharaei@hsu.ac.ir

1977, Blocki *et al.* introduced the first version of the proximity potentials which is known as "proximity 1977 (Prox. 77)". It must be noted that there are adjustable parameters in various parts of the proximity formalism such as the radius parameter R, the surface energy coefficient γ and the universal function $\Phi(s)$ which lead to introduce different versions of the proximity potentials [28–30]. As time went by, several attempts have been done to evaluate the validity of the proximity potentials in order to achieve a reliable and accurate estimation of alpha-decay half-lives of different nuclei. For example, in 2016, the alpha-decay process of 344 isotopes of different elements ranging from $Z = 52$ to $Z = 107$ have been systematically analyzed using 28 versions of the proximity potential model [31]. In that study, Ghodsi *et al.* studied the quality of the selected potential models in reproducing the experimental data of α-decay half-lives. The results of that study reveal that the calculated half-lives using the Prox. 77-set4, Prox. 77-set5 and Dutt 2011 potential models are in very good agreement with experimental data. In another attempt, the authors of ref. [32] performed a systematic study to select an appropriate potential for analyzing the alpha-decay half-lives of Po isotopes, within the mass region $A = 186$–224, using 25 different versions of nuclear proximity potentials. By obtaining the standard deviation of the theoretical half-lives in comparison with the corresponding experimental data, they found that Prox 2003-I with the least standard deviation ($\sigma = 0.620$) provide the most suitable form of the nuclear potential to study the alpha decays. In addition, it is shown that the next low standard deviations are respectively devoted to the Prox. 77 (with $\sigma = 0.630$) and Prox. 66 (with $\sigma = 0.636$) proximity versions.

Recently a systematic study has been carried out on the different α-nuclei systems whose atomic numbers are from $Z = 48$ to $Z = 92$ to analyze the radial behavior of the universal function around the potential barrier of the alpha-daughter nucleus system using the double-folding model with the density-dependent nucleon-nucleon (NN) interactions [33]. The authors of that study introduced a new form of universal function which can be used for proximity potential. They tested the accuracy of the final parameterized form of the $\Phi(s)$ to predict the experimental decay half-lives of different nuclei. The obtained results show that the original version of the proximity potentials along with the proposed universal function can provide acceptable predictions for the nuclear interaction potential of alpha-nuclei system and also decay half-lives [33].

On the basis of the theoretical framework proposed in ref. [33], it is of significant interest to study for the first time the surface energy coefficient γ of proximity formalism using the density-dependent nucleon-nucleon interactions. In order to achieve this aim, we calculate the nuclear potential of 235 alpha-daughter nucleus systems in the range of $61 \leq Z \leq 99$ using the double-folding model with the effective nucleon-nucleon interactions of CDM3Y6-Paris type which fits the saturation properties of cold nuclear matter well. In the next step, using an innovative technique, the values of the surface energy coefficient for alpha-decay of selected nuclei are deduced from the equation of the proximity potential model. By analyzing the behavior of the calculated γ coefficients as a function of the asymmetry parameter $A_s = \frac{N_d+N_\alpha-(Z_d+Z_\alpha)}{N_d+N_\alpha+(Z_d+Z_\alpha)}$, where $N_{d(\alpha)}$ and $Z_{d(\alpha)}$ refer to the neutron and proton numbers of the daughter nuclei and α-particle, respectively, we introduce a new parameterized formula for the surface tension coefficient of the proximity formalism. Ultimately, the quality of the presently obtained formula is tested to predict the experimental data of the α-decay half-lives and fusion cross sections.

This article is organized in the following way. Section 2 gives the relevant details of the theoretical frameworks used to calculate the nuclear potential. Section 3 is devoted to the method for determining the values of the surface energy coefficient. In this section, the calculated results on the alpha-decay of the nuclei under study are displayed and discussed. The conclusions drawn from the present analysis are given in sect. 4.

2 Methodology

As pointed before, the total interaction potential between alpha and daughter nuclei plays a vital role in interpreting the alpha-decay process. It has been well recognized that this potential is defined as the sum of three parts [34]; the long-range repulsive Coulomb potential $V_C(r)$, the short-range attractive nuclear potential $V_N(r)$, and the centrifugal potential $V_l(r)$,

$$V_{\rm tot}(r) = V_C(r) + V_N(r) + V_l(r), \tag{1}$$

where r refers to the separation distance between the mass centers of the α-particle and daughter nucleus. The Coulomb and centrifugal potentials are very well understood and can be calculated accurately. The Coulomb term due to a charge $Z_\alpha e$ interacting with a charge $Z_d e$ can be calculated by following the simple relation

$$V_C(r) = \frac{Z_\alpha Z_d e^2}{r}\,, \tag{2}$$

where Z_α and Z_d denote the atomic numbers of the alpha particle and daughter nuclei, respectively. In eq. (1), the centrifugal term can be defined as

$$V_l(r) = \frac{\hbar^2 l(l+1)}{2\mu r^2}\,, \tag{3}$$

where $\mu = \frac{m_\alpha m_d}{m_\alpha+m_d}$ is the reduced mass of the alpha-daughter nucleus system. Moreover, l is the orbital angular momentum carried away by the emitted α-particle. The nuclear part of interaction potential is not clearly understood. In fact, introducing a comprehensive model to determine the strength of the nuclear interactions between target and projectile is still a challenging problem in the field of theoretical studies of nuclear physics. During recent decades, many efforts have been made to find a simple and accurate form of the nuclear potential [27,35–37]. Here, the double folding and proximity potential models were applied to calculate the nucleus-nucleus potential. They are well known for their simplicity and numerous applications in various theoretical fields.

2.1 The introduction of the proximity model

According to the original version of the proximity potential 1977 [27], the nucleus-nucleus interaction potential can be approximated as follows:

$$V_N(r) = K\Phi\left(\frac{s}{b}\right), \tag{4}$$

where the strength of ths geometrical factor K is given by

$$K = 4\pi b\gamma\overline{R} \tag{5}$$

with the mean curvature radius $\overline{R}$, a kind of "reduced radius" of the two nuclei, reads as

$$\overline{R} = \frac{C_1C_2}{C_1+C_2}\,. \tag{6}$$

Here, C_i denotes the Süssmann' central radii of the fragments which are given by

$$C_i = R_i - \left(\frac{b^2}{R_i}\right), \tag{7}$$

where R_i refers to the effective sharp radius of the α-particle and the daughter nucleus. For calculating this parameter, one can use a semi-empirical formula in terms of mass number A_i as follows [27]:

$$R_i = 1.28A_i^{1/3} - 0.76 + 0.8A_i^{-1/3}\,\mathrm{fm} \quad (i=1,2). \tag{8}$$

In eq. (5), the nuclear surface width (diffuseness) parameter b was taken to be of order of 1 fm. Moreover, γ is the nuclear surface tension coefficient

$$\gamma = \gamma_0\left[1 - k_s\left(\frac{N-Z}{N+Z}\right)^2\right]. \tag{9}$$

Here, N and Z represent the neutron and proton numbers of the parent nucleus, respectively. In this relation, the surface energy constant γ_0 can be defined as

$$\gamma_0 = \frac{a_2}{4\pi r_0^2}\,, \tag{10}$$

where r_0 and a_2 are the nuclear radius constant and the usual liquid drop model surface energy coefficient, respectively. In addition, k_s is the surface asymmetry constant. These constants were first parameterized by Myers and Swiatecki [38] by fitting the experimental binding energies as $\gamma_0 = 1.01734\,\mathrm{MeV}\cdot\mathrm{fm}^{-2}$ and $k_s = 1.79$, respectively. In ref. [39], these values were revised as $\gamma_0 = 0.9517\,\mathrm{MeV}\cdot\mathrm{fm}^{-2}$ and $k_s = 1.7826$. The proximity potential with this revised set of parameters is marked as "Prox. 77". In the original proximity potential 1977, the dimensionless universal function $\Phi(\xi = s/b)$ was parameterized with the following form:

$$\Phi(\xi) = \begin{cases} -\frac{1}{2}(\xi-2.54)^2 - 0.0852(\xi-2.54)^3, & \xi \le 1.2511, \\ -3.437\exp(-\xi/0.75), & \xi \ge 1.2511 \end{cases} \tag{11}$$

where s refers to the separation between the half-density surfaces of the nuclei

$$s = r - C_1 - C_2. \tag{12}$$

2.2 The introduction of the double folding model

The DF model is designed for semimicroscopic calculations of the nucleus-nucleus potential in the frozen density approximation [36,37]. Within the framework of this model, the nuclear potential between two colliding nuclei can be calculated using the following equation:

$$V_{\mathrm{DF}}(\mathbf{R}) = \int \mathrm{d}\mathbf{r}_1 \int \mathrm{d}\mathbf{r}_2 \rho_1(\mathbf{r}_1)\rho_2(\mathbf{r}_2)\upsilon_{NN}(\mathbf{r}_{12} = \mathbf{R} + \mathbf{r}_2 - \mathbf{r}_1). \tag{13}$$

We point out that the calculation of the DF integral requires the knowledge of two main inputs.

i) The density distributions $\rho_i(\mathbf{r}_i)$ of the α and daughter nuclei. We adopt the widely used two-parameter Fermi (2PF) distribution function

$$\rho_\tau(r) = \frac{\rho_{0,\tau}}{1+\exp(\frac{r-R_\tau}{a_\tau})}\,, \tag{14}$$

for the parametrization of the density in the daughter nuclei. Here, $\tau = n, p$ and $\rho_{0,\tau}$ can be determined by normalization conditions so that

$$\int \rho_p(\mathbf{r})\mathrm{d}\mathbf{r} = Z, \tag{15}$$

and

$$\int \rho_n(\mathbf{r})\mathrm{d}\mathbf{r} = N. \tag{16}$$

The half-density radius R_τ and the diffuseness parameter a_τ determine the shape of the density near the nuclear surface. According to ref. [40], the half-density radii of the proton and neutron density distribution for a nucleus (Z, N) can be given by

$$R_p = 1.322Z^{1/3} + 0.007N + 0.022\,\mathrm{fm}, \tag{17}$$

and

$$R_n = 0.953N^{1/3} + 0.015Z + 0.774\,\mathrm{fm}. \tag{18}$$

The diffuseness parameters of the proton neutron density distribution for a nucleus (Z, N) can be represented as [40]

$$a_p = 0.449 + 0.071\left(\frac{Z}{N}\right)\mathrm{fm}, \tag{19}$$

and

$$a_n = 0.446 + 0.072\left(\frac{N}{Z}\right)\mathrm{fm}. \tag{20}$$

Note that we use the following Gaussian form to parameterize the density distribution of the alpha nucleus:

$$\rho_\alpha(r) = 0.4229\exp(-0.7024r^2)\,\mathrm{fm}^{-3}. \tag{21}$$

ii) The central part υ_{NN} which evaluates the strength of the nucleon-nucleon interactions. Here, we employe the density-dependent M3Y-Paris effective nucleon-nucleon interactions with a finite-range approximation for it's exchange part [41].

In the present study, the half-life of the parent nucleus against the split into an alpha particle and a daughter nucleus is calculated using the following relation:

$$T_{1/2} = \frac{h \ln 2}{2E_{\upsilon} P_0 P}, \tag{22}$$

where the penetration probability P through the Coulomb barrier can be determined within the framework of the Wentzel-Kramers-Brillouin (WKB) approximation as follows:

$$P = \exp\left[-\frac{2}{\hbar} \int_{R_a}^{R_b} \sqrt{2\mu(V_{\rm tot}(r) - Q_\alpha)} \mathrm{d}r \right], \tag{23}$$

where Q_α is the released energy of the emitted α-particle. Moreover, R_a and R_b refer to the physical turning points and are given by

$$V_{\rm tot}(R_a) = Q_\alpha = V_{\rm tot}(R_b). \tag{24}$$

In the calculation of the α-decay half-life, the zero point vibration energy E_υ can be obtained from the assault frequency

$$E_\upsilon = \frac{1}{2}\hbar\omega = \frac{1}{2}h\nu. \tag{25}$$

According to ref. [42], the following law was found for calculating the zero point vibration energies for the α-decays:

$$\begin{aligned} E_\upsilon &= 0.1045 Q_\alpha \,\mathrm{MeV}, \\ &\quad \text{for even}(Z)\text{-even}(N) \text{ parent nuclei} \\ &= 0.0962 Q_\alpha \,\mathrm{MeV}, \\ &\quad \text{for odd}(Z)\text{-even}(N) \text{ parent nuclei} \\ &= 0.0907 Q_\alpha \,\mathrm{MeV}, \\ &\quad \text{for even}(Z)\text{-odd}(N) \text{ parent nuclei} \\ &= 0.0767 Q_\alpha \,\mathrm{MeV}, \\ &\quad \text{for odd}(Z)\text{-odd}(N) \text{ parent nuclei}. \end{aligned} \tag{26}$$

The α preformation factor P_0 in eq. (22) is an indispensable quantity for the calculation. This factor can supply the information of the nuclear structure, see for example refs. [43–45]. The preformation factor was obtained as 0.43 for even-even nuclei, 0.35 for odd-A nuclei and 0.18 for odd-odd nuclei [46].

3 Calculations and results

From the theoretical viewpoint, it is important to know that the surface energy coefficient γ is one of the most influential parameters in studying the alpha-decay of heavy and super-heavy nuclei within the framework of the proximity potential model, see for example refs. [47–49]. In recent years, several attempts have been made to indicate how much this coefficient can alter the results related to the interaction potential between the emitted α-particle and the daughter nucleus, the α-decay penetration probability through the potential barrier and result in the alpha-decay half-lives [47–49]. The importance of the coefficient gamma in analyzing the heavy-ion fusion reactions and cluster radioactivity of nuclei has also been successfully explored in several papers, see for example refs. [30,50–53]. We are here interested in investigating the nuclear surface energy coefficient γ of the proximity formalism by considering the effective density-dependent nucleon-nucleon interactions in an alpha-daughter system. The main goal of the present study is to introduce an analytical formula of the coefficient γ for these types of interacting systems. In the following, more details regarding the present method of calculating the values of this coefficient will be provided for α-decay ground-state–to–ground-state transitions of 235 heavy nuclei with a wide range of atomic numbers $61 \leq Z_P \leq 99$. It must be noted that the majority of the ground-state α-emitters considered here are spherical or slightly deformed nuclei [54]. Generally, we consider the alpha-decay process of 74 even(Z)-even(N), 74 even(Z)-odd(N), 58 odd(Z)-even(N) and 29 odd(Z)-odd(N) parent nuclei. The experimental data of the α-decay half-lives and energy released are available for our selected alpha emitters.

Based on the realistic density-dependent effective CDM3Y6-Paris NN interactions, we have initially computed the interaction potential between α cluster and the daughter nucleus using the microscopic DF potential at the contact point distance $r = R_t = R_1 + R_2$. By establishing a logical connection between the proximity and DF potential models, namely eqs. (4) and (13), one can determine the values of the surface energy coefficient γ with the presently suggested equation

$$\gamma = \frac{V_N(s)}{4\pi b \overline{R} \Phi(s)}. \tag{27}$$

To calculate the universal function $\Phi(s)$, it is necessary to say that the shape of this function must be like that of the nucleus-nucleus potential. Therefore, herein, we use a new universal function [55], which is obtained by using the DF model with density-dependent nucleon-nucleon interaction (CDM3Y6), as follows:

$$\Phi(s) = \frac{p_1}{1 + \exp(\frac{s+p_2}{p_3})}, \tag{28}$$

where the values of p_1, p_2 and p_3 constants are equal to -17.72, 1.30 and 0.854, respectively [55]. Note, the calculations of $\Phi(s)$ have also been performed at the touching configuration. The knowledge of the values of the surface energy coefficient γ allows one to analyze the variation trend of this coefficient with asymmetry parameter A_s. If one looks on the nuclear surface tension formula, eq. (9), one notices that the asymmetry dependence of the proximity potential enters via the coefficient γ. In this situation, we can conclude that the nuclear surface tension coefficient plays a significant role in the calculations of the nuclear potential and result in the calculations of the Coulomb barrier. In fig. 1, we display the variation of γ (in MeV/fm^2) as a function of the squared asymmetry parameter A_s^2. The calculated values contain all 235 alpha-decay processes. It is shown that the values of the calculated

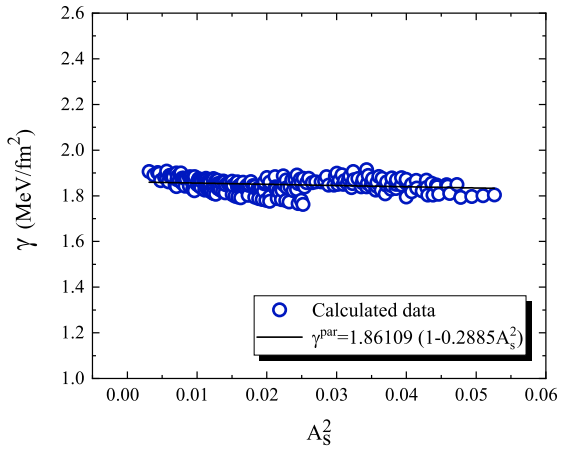

Fig. 1. The variation trend of the calculated values of the surface energy coefficient γ from the DF model with the effective density-dependent CDM3Y6-Paris interaction as a function of the squared asymmetry parameter A_s^2. The present fitted $\gamma(A_s)$, eq. (29), correspond to the solid line.

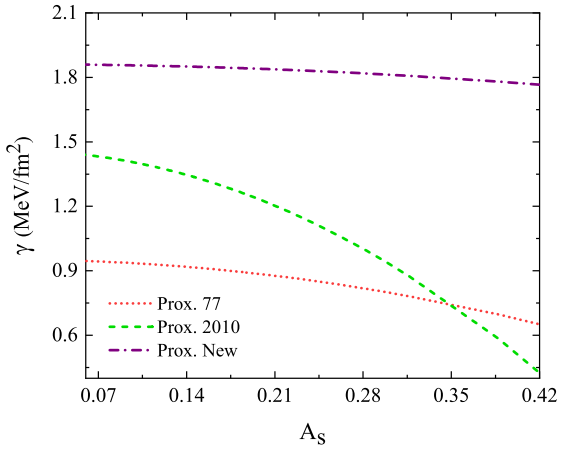

Fig. 2. Dependence of the surface energy coefficients used in the Prox. 77 and Prox. 2010 models on the asymmetry of the α-daughter system compared with those obtained by the present formula (29).

gamma coefficient decrease linearly with increase of the parameter A_s^2. One can parameterize the linear trend of the surface energy coefficients using the following relation:

$$\gamma(A_s) = \alpha\big[1 - \beta A_s^2\big], \tag{29}$$

where the extracted values of (α, β) constants are $(1.86109\,\mathrm{MeV}\cdot\mathrm{fm}^{-2}, 0.2885)$ based on the DF model with the density-dependent NN interaction of the CDM3Y6-type. It is observed that the values of the coefficient γ for all considered decays are localized around the fitted line. Under these conditions, the fitted line can effectively provide a complete description of the nuclear surface tension of various α-nuclei systems.

To gain further insight, in fig. 2, we compare the results of eq. (29) with those calculated by two versions of the surface energy coefficient used in the Prox. 77 and Prox. 2010 potential models as a function of the asymmetry parameter A_s. In the latter potential, the surface energy coefficient γ_0 and the surface-asymmetry constant k_s were parameterized as $\gamma_0 = 1.460734\,\mathrm{MeV}\cdot\mathrm{fm}^{-2}$ and $k_s = 4.0$ [56]. As can be seen from fig. 2, the presently suggested formula (29) indicates a weaker dependence of the values of the gamma coefficient on the asymmetry of the alpha-daughter systems than those used in the original and latest versions Prox. 77 and Prox. 2010. In addition, our comparison reveals that the nuclear surface energy coefficient from the Prox. 2010 has a stronger dependence on the parameter A_s of the alpha-daughter system. Note that we have performed the calculations of fig. 2 for an expanded range of the asymmetry parameter to give a better understanding of the decreasing trend of the coefficient γ calculated by various potential models especially "Prox. New".

By imposing the proposed formula in the proximity formalism one can obtain the strength of the nuclear potential between α-particle and daughter nuclei. We mark this modified form of the proximity potential as "Prox. New". Since the nuclear proximity potential depends directly on the surface energy coefficient, we can conclude that the interaction potentials calculated by the Prox. 77 and Prox. 2010 models will be less attractive for different asymmetries in comparison with the one obtained from the presently modified proximity potential. To further understand the role of the surface tension effects, in fig. 3, we plot the behavior of the total interaction potential $V_{\mathrm{tot}}(r)$ (in MeV) against the center-to-center distance r (in fm) of the participant nuclei in alpha process using the Prox. New potential model for two alpha-decays $^{182}\mathrm{Hg} \rightarrow {}^{178}\mathrm{Pt} + {}^{4}\mathrm{He}$ and $^{221}\mathrm{Pa} \rightarrow {}^{217}\mathrm{Ac} + {}^{4}\mathrm{He}$, for example. The calculations of the figure have been performed for angular momentum $l = 0$. It also includes the results of the original proximity potential 1977 for comparison. The short dashed line in each panel of this figure denotes the characteristic quantity Q_α-value. It has to be mentioned that the values of the surface energy coefficient calculated by the analytical formula (29) are equal to $\gamma = 1.85324\,\mathrm{MeV}\cdot\mathrm{fm}^{-2}$ and $\gamma = 1.84436\,\mathrm{MeV}\cdot\mathrm{fm}^{-2}$ for the α-decay of ^{182}Hg and ^{221}Pa parent nuclei, respectively. While the coefficient γ of the original proximity potential 1977 yields the values of $\gamma = 0.92691\,\mathrm{MeV}\cdot\mathrm{fm}^{-2}$ and $\gamma = 0.89886\,\mathrm{MeV}\cdot\mathrm{fm}^{-2}$ for these processes, respectively. From fig. 3, we see that the imposing of the presently suggested formula in the proximity formalism causes the height and also the width of the Coulomb barrier shift toward the lower values. The obtained values for the barrier height V_B and barrier curvature $\hbar\omega_B$ based on the original and modified forms of the proximity potential for both selected alpha-decays are listed in table 1. Depending on the table, one can find out that the calculated values of V_B and $\hbar\omega_B$ resulting from the Prox. New potential model reduce as much as 1.09 MeV and 0.43 MeV for the case

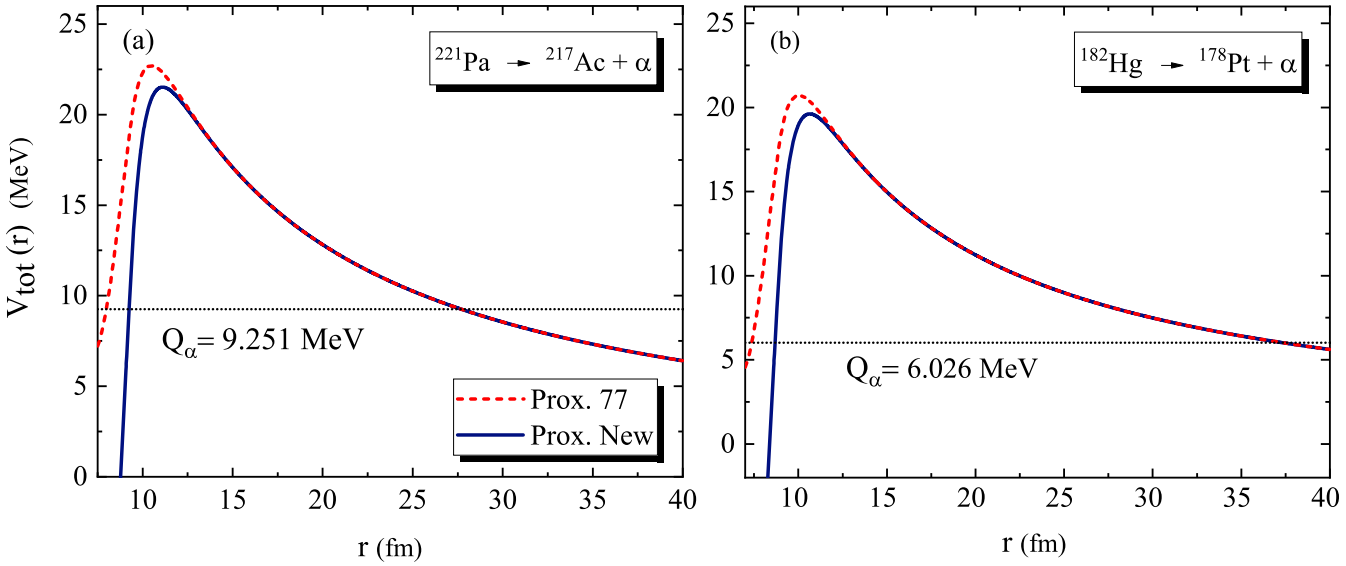

Fig. 3. The interaction potentials for alpha-decays from (a) ^{221}Pa and (b)^{182}Hg parent nuclei based on the Prox. 77 and Prox. New potential models. In each panel, the experimental value of Q_α is shown by using the horizontal dotted line.

Table 1. The obtained values of the Coulomb barrier height V_B and barrier curvature $\hbar\omega_B$ using the original and modified form of the proximity potential for α-decay ^{182}Hg and ^{221}Pa parent nuclei.

α-decay	Prox. 77		Prox. New	
	V_B (MeV)	$\hbar\omega_B$ (MeV)	V_B (MeV)	$\hbar\omega_B$ (MeV)
^{182}Hg → ^{178}Pt + ^{4}He	20.70	5.27	19.61	4.84
^{221}Pa → ^{217}Ac + ^{4}He	22.70	5.34	21.51	5.02

of ^{182}Hg → ^{178}Pt + ^{4}He and as much as 1.19 MeV and 0.29 MeV for the case of ^{221}Pa → ^{217}Ac + ^{4}He in comparison with the Prox. 77 model. In this situation, one can expect that these changes affect the penetration probabilities and result in the theoretical half-lives for the studied processes.

The theoretical half-lives provided by the above mentioned proximity potentials are listed in table 2 which includes the results of the Prox. 77 and Prox. New models. In these tables, we have displayed the values of $T_{1/2}$ for ground-state–to–ground-state transition of 75 alpha-decays, for example. The third and fourth columns show the existing experimental data of the released energies Q_α as well as half-lives of the parent nuclei. By comparing between the theoretical and experimental data of $T_{1/2}$, one can find out that the modified form of the proximity potential is suitable for calculating the half-life of the α-decay. In order to further examine the predictive ability of the mentioned nuclear proximity potentials, in fig. 4, the absolute difference between the calculated and experimental values of $\log_{10}(T_{1/2})$ is presented as a function of the neutron number of different daughter nuclei using Prox. 77 and Prox. New potential models. As can be seen from figure, for most of the considered alpha transitions caused by the modified form of the proximity potential the difference is within 0.5 order of magnitude, whereas the results of original proximity potential 1977 have been scattered around unity. Only a few cases lie above (below)

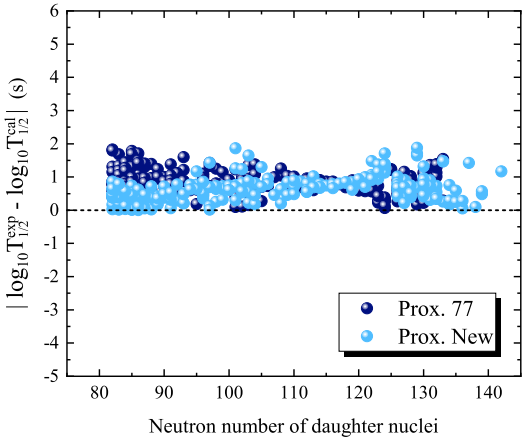

Fig. 4. The absolute difference between the predicted alpha half-lives and the experimental data using the original and modified forms of the proximity potential against the neutron number of daughter nuclei.

these order of magnitudes. These results imply that the presently suggested form of the proximity potential provides the better predictions for theoretical values of the alpha-decay half-lives for the studied α-emitters.

Table 2. Comparison of the calculated alpha-decay half-lives using the Prox. New and Prox. 77 potential models with the corresponding experimental data for the emission of the alpha particle from some of the selected isotopes. The theoretical half-lives are calculated for zero angular momentum transfers.

Parent nuclei	Z_p	$Q_\alpha^{\exp}$ (MeV)	$T_{1/2}^{\exp}$ (s)	$T_{1/2}^{\text{cal(Prox. New)}}$ (s)	$T_{1/2}^{\text{cal(Prox. 77)}}$ (s)
^{146}Sm	62	2.550	3.30E+15	3.06E+15	6.78E+16
^{147}Sm	62	2.311	3.36E+18	6.88E+18	1.63E+20
^{147}Eu	63	2.991	9.46E+10	2.84E+11	5.98E+12
^{148}Eu	63	2.724	5.00E+14	4.83E+14	1.09E+16
^{148}Gd	64	3.293	2.40E+09	1.63E+09	3.38E+10
^{149}Gd	64	3.099	1.86E+11	1.33E+11	2.90E+12
^{150}Gd	64	2.822	5.60E+13	6.52E+13	1.54E+15
^{151}Gd	64	2.692	1.10E+15	2.74E+15	6.73E+16
^{152}Gd	64	2.219	3.40E+21	6.16E+21	1.74E+23
^{152}Ho	67	4.529	1.20E+03	7.56E+02	1.40E+04
^{153}Ho	67	4.038	2.40E+05	3.16E+05	6.60E+06
^{152}Er	68	4.955	1.10E+01	4.61E+00	8.19E+01
^{153}Er	68	4.823	7.10E+01	2.91E+01	5.33E+02
^{154}Er	68	4.301	4.80E+04	1.83E+04	3.80E+05
^{154}Yb	70	5.484	4.40E-01	1.54E-01	2.74E+00
^{155}Yb	70	5.353	2.00E+00	7.97E-01	1.46E+01
^{156}Yb	70	4.836	2.60E+02	1.93E+02	4.00E+03
^{157}Yb	70	4.646	8.00E+03	2.90E+03	6.30E+04
^{158}Yb	70	4.199	3.00E+06	1.10E+06	2.68E+07
^{155}Lu	71	5.831	8.90E-02	2.08E-02	3.64E-01
^{158}Lu	71	4.815	1.20E+03	2.65E+03	5.91E+04
^{159}Lu	71	4.559	3.00E+04	2.98E+04	7.09E+05
^{158}Hf	72	5.430	6.30E+00	2.29E+00	4.69E+01
^{159}Hf	72	5.252	4.70E+01	2.13E+01	4.56E+02
^{161}Hf	72	4.724	1.40E+04	1.16E+04	2.83E+05
^{162}Hf	72	4.443	4.00E+05	3.76E+05	9.92E+06
^{160}W	74	6.098	9.00E-02	2.80E-02	5.59E-01
^{163}W	74	5.547	6.70E+00	7.55E+00	1.71E+02
^{164}W	74	5.303	2.50E+02	7.33E+01	1.76E+03
^{166}W	74	4.883	5.50E+04	1.06E+04	2.84E+05
^{161}Os	76	7.065	6.40E-04	1.04E-04	1.90E-03
^{162}Os	76	6.806	1.90E-03	5.07E-04	9.78E-03
^{163}Os	76	6.675	5.50E-03	1.94E-03	3.84E-02
^{165}Os	76	6.345	6.50E-02	2.86E-02	6.09E-01
^{170}Os	76	5.569	5.90E+01	3.02E+01	7.75E+02
^{169}Ir	77	6.266	4.00E-01	1.29E-01	2.97E+00
^{170}Ir	77	6.203	1.10E+00	5.32E-01	1.24E+01
^{172}Ir	77	5.997	2.10E+00	3.40E+00	8.32E+01
^{177}Ir	77	5.082	5.00E+04	8.86E+05	2.78E+04
^{173}Pt	78	6.358	4.44E-01	3.35E+00	1.40E-01
^{175}Pt	78	6.178	3.95E+00	1.66E+01	6.66E-01
^{177}Pt	78	5.643	1.86E+02	3.98E+03	1.37E+02
^{174}Au	79	6.713	1.20E-01	3.95E-02	9.21E-01
^{175}Au	79	6.62	2.00E-01	3.39E-02	8.06E-01

Table 2. Continued.

Parent nuclei	Z_p	$Q_\alpha^{\exp}$ (MeV)	$T_{1/2}^{\exp}$ (s)	$T_{1/2}^{\text{cal(Prox. New)}}$ (s)	$T_{1/2}^{\text{cal(Prox. 77)}}$ (s)
^{178}Au	79	6.085	1.00E+01	9.65E+00	2.65E+02
^{183}Au	79	5.465	7.78E+03	2.28E+03	7.56E+04
^{173}Hg	80	7.375	9.10E-04	2.68E-04	5.70E-03
^{178}Hg	80	6.606	5.00E-01	6.95E-02	1.78E+00
^{179}Hg	80	6.443	2.00E+00	4.00E-01	1.07E+01
^{180}Hg	80	6.287	6.10E+00	1.14E+00	3.18E+01
^{181}Hg	80	6.168	1.00E+01	4.81E+00	1.38E+02
^{183}Hg	80	6.038	8.03E+01	1.57E+01	4.69E+02
^{186}Hg	80	5.236	5.20E+05	7.88E+04	3.07E+06
^{189}Po	84	7.694	3.80E-03	5.03E-04	1.25E-02
^{195}Po	84	6.755	4.94E+00	7.04E-01	2.30E+01
^{212}Po	84	8.99	2.99E-07	2.89E-08	5.54E-07
^{213}Po	84	8.571	3.72E-06	4.54E-07	9.74E-06
^{215}Po	84	7.562	1.78E-03	3.68E-04	1.06E-02
^{216}Po	84	6.942	1.44E-01	3.46E-02	1.22E+00
^{217}Po	84	6.699	1.53E+00	3.93E-01	1.52E+01
^{195}Rn	86	7.694	7.00E-03	2.44E-03	6.96E-02
^{196}Rn	86	7.617	4.70E-03	2.92E-03	8.51E-02
^{197}Rn	86	7.415	5.40E-02	1.88E-02	5.80E-01
^{198}Rn	86	7.349	6.50E-02	2.13E-02	6.71E-01
^{202}Rn	86	6.77	1.15E+01	2.44E+00	9.36E+01
^{201}Fr	87	7.515	6.20E-02	1.73E-02	5.60E-01
^{203}Fr	87	7.274	5.50E-01	1.08E-01	3.80E+00
^{215}Fr	87	9.54	8.60E-08	1.84E-08	3.59E-07
^{216}Fr	87	9.174	7.00E-07	3.21E-07	6.89E-06
^{216}Th	90	8.072	2.60E-02	5.44E-02	1.56E-03
^{220}Th	90	8.95	9.77E-06	1.00E-04	3.70E-06
^{214}Pa	91	8.27	1.70E-02	1.18E-01	3.40E-03
^{221}Pa	91	9.251	5.90E-06	4.68E-05	1.77E-06
^{224}U	92	8.62	8.40E-04	4.87E-03	1.42E-04
^{226}U	92	7.701	2.68E-01	5.18E+00	1.06E-01

For a better understanding, we have also calculated the root-mean-square (rms) deviations σ of logarithm values of the theoretical half-lives resulting from the original and modified forms of the proximity potential in comparison with the corresponding experimental data for all 235 alpha-decay processes. Herein, the rms deviation are calculated using the following definition:

$$\sigma = \sqrt{\frac{1}{N}\sum_{i=1}^{N}\left[\log_{10}\left(T_{1/2i}^{\text{theor.}}\right) - \log_{10}\left(T_{1/2i}^{\text{expt.}}\right)\right]^2}, \quad (30)$$

where N is the number of parent nuclei used for evaluation of the σ value. It is found that the rms deviation deduced from the proximity model with the presently obtained formula (29) is $\sigma = 0.7910$, whereas the rms deviation resulting from the original proximity 1977 is $\sigma = 0.9746$. That is, our analytical formula generates the smaller value of the σ value. Using the Prox. New potential model, the rms deviations were recalculated for even-even, even-odd, odd-even and odd-odd nuclei. Our results reveal that the calculated rms deviations for even-even, odd-even, even-odd and odd-odd nuclei are 0.6783, 0.7385, 0.8240 and 1.0359, respectively. These values imply that the half-lives predicted for even-even are very close to the corresponding experimental data.

3.1 Analysis of the shell closure effects

It will be interesting to see whether the proximity formalism with new proposed form of the surface energy coefficient γ can reproduce the shell effects on α transitions. For this purpose, within the Prox. New potential model,

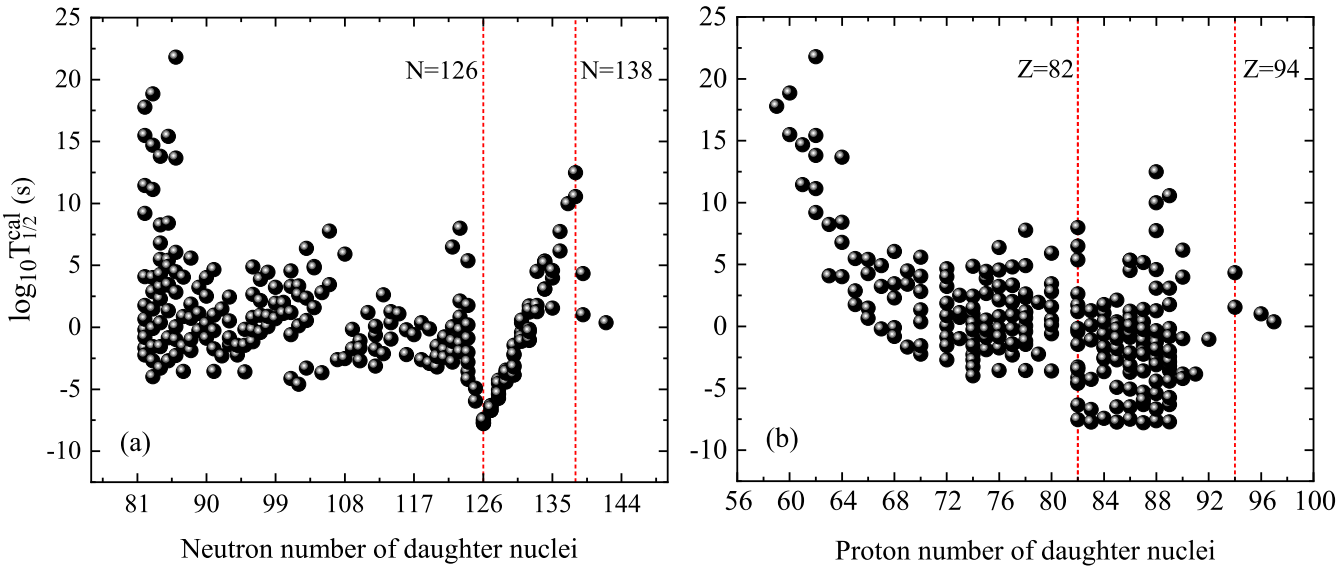

Fig. 5. The behavior of the logarithmic values of the calculated half-lives using the proximity potential accompanied by the analytical form of the parameter γ, eq. (29), as a function of the neutron number N (left panel) and proton number Z (right panel) of the daughter nuclei. The α-decay half-lives increase rapidly between $N = 126$ and $N = 138$, whereas a small stability excess appears from the half-life curve between $Z = 82$ and $Z = 94$. The vertical red lines for both panels show the range for these trends.

the variation trend of the α-decay half-lives as a function of the neutron number of daughter nuclei is shown in fig. 5 (left panel). As can be seen in the figure, the half-life presents vibrations with increasing neuron number before $N = 126$. A clear minimum occurs at $N = 126$ which is a neutron magic number. Between $N = 126$ and $N = 138$, the half-life increases rapidly and almost linearly. Then, the values of this quantity decrease again. This is because of the large gap above the magic number $N = 126$. In fig. 5 (right panel), we display the computed $\log_{10}(T_{1/2})$ values *versus* proton number Z of the daughter nuclei. Before $Z = 82$, the α-decay half-lives decrease with increasing the proton number Z. The trend of the curve do not show a visible gap for nuclei with $Z = 82$ which is a well-known proton magic number. A comparison of the behavior of the calculated half-lives as a function of the neutron and proton numbers emphasizes that the proton magic number $Z = 82$ may have smaller effects than the neutron number $N = 126$ for the alpha-decay properties. It is difficult to identify the real cause for this phenomenon, but, nevertheless a similar result can be deduced from the variations trend of the experimental α-decay energy in terms of the neutron and proton numbers N and Z.

3.2 Search for validity of the Geiger-Nuttall alpha-decay law

It is well recognized that the Geiger-Nuttall (G-N) law relates the partial alpha-decay half-life of a radioactive nucleus with the released energy of the emitted α-particles [57]. Herein, we would like to study the G-N plots for α-decay from various isotopes using the proximity potential with new analytical formula of the surface energy coefficient γ. In fig. 6, these plots have been drawn for $^{161-174}$Os (with $Z = 76$), $^{173-185}$Au (with $Z = 79$), $^{173-188}$Hg (with $Z = 80$), $^{202-222}$Ra (with $Z = 88$), $^{207-225}$Ac (with $Z = 89$) and $^{210-230}$Th (with $Z = 90$) isotopes, for example. We find out that the plots are straight lines with different slopes and intercepts. The linearity of the G-N plots reveals the validity of the Prox. New potential model. In fig. 6, the G-N plots for the cluster ^{4}He from different isotopes Os, Au, Hg, Ra, Ac and Th are also given for the Prox. 77 potential model and it is also found to be linear with different slopes and intercepts. We would like to mention that the G-N plots based on the Prox. 77 nuclear potential model are lying higher than those obtained by the Prox. New potential model. To formulate the behavior of the calculated decimal logarithmic half-lives as a function of the total energy of the alpha-decay process $Q_\alpha^{-1/2}$ (in MeV$^{-1/2}$), we arrived at an equation as follows:

$$\log_{10} T_{1/2} = AQ_\alpha^{-1/2} + B, \tag{31}$$

where the values of slope A and intercept B for α-decay from various isotopes based on the Prox. 77 and Prox. New potential models are listed in table 3.

3.3 Quantitative analysis of the α-capture cross sections

Another interesting subject in the context of theoretical studies of nuclear physics is to describe simultaneously the α-capture and α-decay reactions using the same interaction potential model [58–60]. It turns out that the distance between the α-particle and nucleus is reduced during the

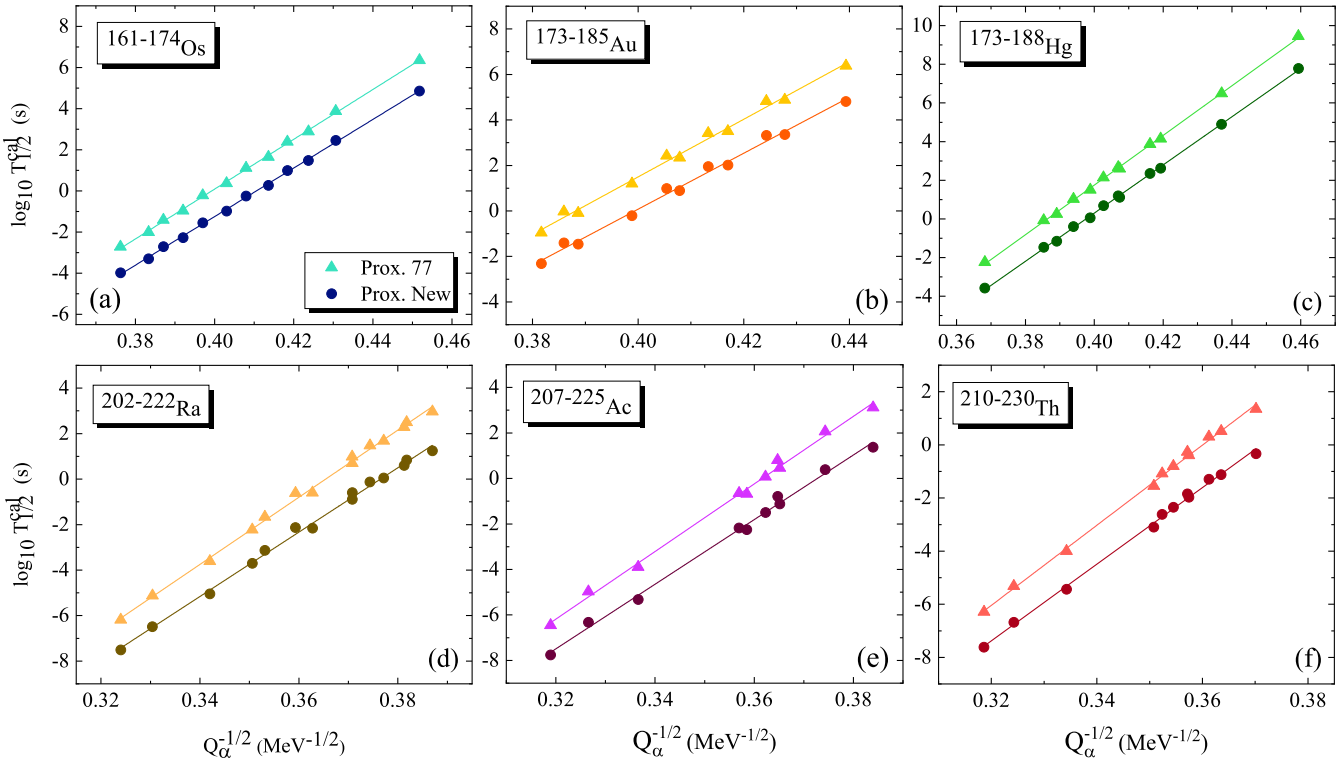

Fig. 6. Geiger-Nuttall plot of $\log_{10}(T_{1/2})$ values *versus* $Q_\alpha^{-1/2}$ for the emission of α-particle from (a) $^{161-174}$Os, (b) $^{173-185}$Au, (c) $^{173-188}$Hg, (d) $^{202-222}$Ra, (e) $^{207-225}$Ac, (f) $^{210-230}$Th parent nuclei using the Prox. New (solid circles) and Prox. 77 (up-pointing triangles) potential models. $T_{1/2}$ is in seconds.

Table 3. The slopes A and intercepts B of the G-N plots for α-decay from different isotopes based on the Prox. New and Prox. 77 potential models.

Parent nuclei	Prox. 77		Prox. New	
	A (MeV$^{1/2}$s)	B (s)	A (MeV$^{1/2}$s)	B (s)
$^{210-230}$Th	−54.30	150.81	−53.49	144.11
$^{207-225}$Ac	−53.72	148.57	−52.93	142.01
$^{173-185}$Au	−49.14	126.61	−49.10	122.95
$^{161-174}$Os	−48.36	121.13	−48.49	118.12
$^{173-188}$Hg	−49.62	128.44	−49.54	124.62
$^{202-222}$Ra	−53.94	147.63	−53.26	141.48

fusion process, whereas the distance increases in the alpha-decay of a parent nucleus. This implies that the fusion reaction between α-particle and nucleus (α-capture reaction) proceeds in the opposite direction to the α-decay. Under these conditions, one can expect that the knowledge of the α-nucleus potential plays a key role in characterizing both mentioned reactions. The present study indicates that the proximity potential supplemented with the presently obtained formula for the coefficient γ is able to reproduce the evaluated α-decay half-lives. It is therefore interesting to investigate the validity of the modified form of the proximity potential for reproducing the sub-barrier fusion cross sections. In fig. 7, we compare the experimental fusion cross sections for alpha induced reactions on ^{40}Ca, ^{48}Ti, ^{51}V, ^{59}Co, ^{63}Cu, ^{93}Nb, ^{154}Sm and ^{162}Dy nuclei with those calculated by using the Prox. New potential model. It is remarkable that the one-dimensional barrier penetration model (1D-BPM) [34] is used to evaluate the energy-dependent behavior of the fusion cross sections between and α-particle and a target nucleus. We see that our Prox. New model accurately describes the fusion data of the studied α-capture reactions. Note that the fusion cross sections of similar and different α-capture systems have been theoretically analyzed in the framework of the proximity potentials 1977 and 2010. The obtained results reveal that the original proximity potential fails

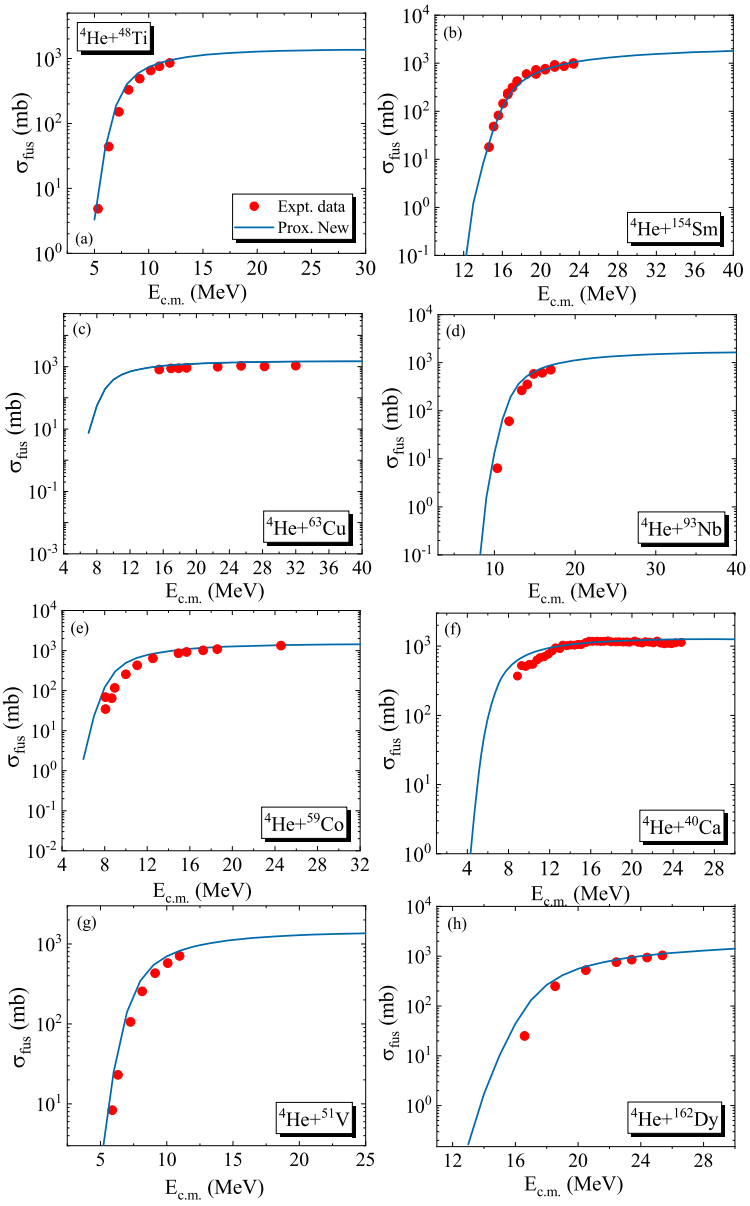

Fig. 7. The energy-dependent behavior of the experimental fusion cross sections for the reactions (a) $\alpha + {}^{48}$Ti [62], (b) $\alpha + {}^{154}$Sm [63], (c) $\alpha + {}^{63}$Cu [64], (d) $\alpha + {}^{93}$Nb [65], (e) $\alpha + {}^{59}$Co [66], (f) $\alpha + {}^{40}$Ca [67], (g) $\alpha + {}^{51}$V [62] and (h) $\alpha + {}^{162}$Dy [68] compared with the 1D-BPM calculations based on the Prox. New potential model.

to reproduce the experimental fusion cross sections with an acceptable accuracy, whereas its modified forms do a better job [28–30,61].

4 Summary and conclusions

In this paper we have applied the DF model with the realistic density-dependent NN interaction to a systematic investigation of the surface energy coefficient γ of the nuclear proximity potential between alpha-particle and nuclei. In DF model, the NN interaction is selected as CDM3Y6-Paris type. We calculate the nuclear DF potentials of 235 α-nuclei systems whose proton numbers are $Z = 61$–99. Then, we obtain the values of the calculated γ by introducing a logical connection between the DF proximity potential models at the touching point of the reacting nuclei. The main conclusions of the present paper can be summarized as follows.

i) We have succeeded to present a new form of the nuclear surface tension coefficient γ of the proximity formalism by fitting the calculated values of this coefficient for different alpha-nuclei systems. We conclude that the presently obtained formula (29) has a weaker dependence

on the asymmetry of the reacting nuclei than the one used in the proximity potentials 1977 and 2010. On the other hand, the results of the present survey show that a less dependence on the asymmetry of the reacting nuclei gives rise to form a lower and thinner barrier in the framework of the proximity formalism. Since this modification leads to achieve more accurate predictions for the experimental data of $T_{1/2}$ in the presently studied α-nucleus systems, one may find out some advantages of the presently introduced proximity model in comparison with its older versions.

ii) We test the quality of the suggested form of the surface energy coefficient γ by calculating the alpha-decay half-lives of all 235 parent nuclei from ground-state–to–ground-state transitions in comparison with the experimental data. The results show that the half-lives calculated by the Prox. New potential model are in good agreement with the experimental half-life values, with a difference of about 0.5 order of magnitude. Moreover, it appears that the present proximity potential worked better for even-even isotopes than for the other ones, because there is no the angular momentum uncertainty for such α-transitions. The theoretical results evaluated using the Prox. New model were compared with those obtained by the Prox. 77 model. Our comparison showed that the rms deviation of the decimal logarithm of the half-lives based on the Prox. New model ($\sigma = 0.7910$) has a smaller value than the original version of the proximity formalism ($\sigma = 0.9746$).

iii) In the present study, the validity of the analytical formula of the nuclear surface tension coefficient γ, eq. (29), has been examined using the G-N plots. Within the framework of the Prox. New potential model, it is shown that the calculated values of the partial α-decay half-lives for the ground-state–to–ground-state transitions follow a regular linear trend as a function of $Q_\alpha^{-1/2}$. This implies that the G-N law can be verified in different isotopes chains using the modified form of the proximity potential.

iv) In the framework of the Prox. New model we have analyzed the energy-dependent behavior of the fusion cross sections for alpha-induced reactions on ^{40}Ca, ^{48}Ti, ^{51}V, ^{59}Co, ^{63}Cu, ^{93}Nb, ^{154}Sm and ^{162}Dy nuclei. A comparison with fusion studies shows that the Prox. New model has a good predictive power for α-decay studies and also for the prediction of the α-nucleus fusion cross sections at energies around and below the barrier.

Data Availability Statement This manuscript has no associated data or the data will not be deposited. [Authors' comment: All data generated during this study are contained in this published article.]

Publisher's Note The EPJ Publishers remain neutral with regard to jurisdictional claims in published maps and institutional affiliations.

References

1. D.S. Delion, S. Peltonen, J. Suhonen, Phys. Rev. C **73**, 014315 (2006).
2. P.R. Chowdhury, C. Samanta, D.N. Basu, Phys. Rev. C **73**, 014612 (2006).
3. W.M. Seif, Phys. Rev. C **74**, 034302 (2006).
4. D.N. Basu, J. Phys. G: Nucl. Part. Phys. **30**, B35 (2004).
5. S. Hofmann, G. Münzenberg, Rev. Mod. Phys. **72**, 733 (2000).
6. Yu.Ts. Oganessian *et al.*, Nature (London) **400**, 242 (1999).
7. E. Rutherford, Philos. Mag. **47**, 109 (1899).
8. E. Rutherford, H. Geiger, Proc. R. Soc. London Ser. A **81**, 141 (1908).
9. E. Rutherford, T. Royds, Philos. Mag. **17**, 281 (1908).
10. Yu.Ts. Oganessian *et al.*, Phys. Rev. C **69**, 021601(R) (2004).
11. Yu.Ts. Oganessian *et al.*, Phys. Rev. C **69**, 054607 (2004).
12. Yu.Ts. Oganessian *et al.*, Phys. Rev. C **70**, 064609 (2004).
13. Yu.Ts. Oganessian *et al.*, Phys. Rev. C **71**, 029902(E) (2005).
14. Yu.Ts. Oganessian *et al.*, Phys. Rev. C **72**, 034611 (2005).
15. Yu.Ts. Oganessian *et al.*, Phys. Rev. C **74**, 044602 (2006).
16. S. Hofmann *et al.*, Eur. Phys. J. A **32**, 251 (2007).
17. Yu.Ts. Oganessian *et al.*, Phys. Rev. C **76**, 011601(R) (2007).
18. K. Morita *et al.*, J. Phys. Soc. Jpn. **76**, 045001 (2007).
19. J.C. Pei, F.R. Xu, Z.J. Lin, E.G. Zhao, Phys. Rev. C **76**, 044326 (2007).
20. A.N. Andreyev *et al.*, Eur. Phys. J. A **6**, 381 (1999).
21. G.Z. Gamow, Phys. **51**, 204 (1928).
22. E.U. Condon, R.W. Guerney, Nature **122**, 439 (1928).
23. E.U. Condon, R.W. Guerney, Phys. Rev. **33**, 127 (1929).
24. H.F. Zhang, W. Zuo, J.Q. Li, G. Royer, Phys. Rev. C **74**, 017304 (2006).
25. H.F. Zhang, G. Royer, Phys. Rev. C **76**, 047304 (2007).
26. P.R. Chowdhury, D.N. Basu, C. Samanta, Phys. Rev. C **75**, 047306 (2007).
27. J. Blocki, J. Randrup, W.J. Swiatecki, C.F. Tsang, Ann. Phys. (N.Y.) **105**, 427 (1977).
28. I. Dutt, R.K. Puri, Phys. Rev. C **81**, 044615 (2010).
29. I. Dutt, R.K. Puri, Phys. Rev. C **81**, 064609 (2010).
30. I. Dutt, R.K. Puri, Phys. Rev. C **81**, 047601 (2010).
31. O.N. Ghodsi, A. Daei-Ataollah, Phys. Rev. C **93**, 024612 (2016).
32. K.P. Santhosha, Indu Sukumaran, Eur. Phys. J. A **53**, 246 (2017).
33. G.L. Zhang, H.B. Zheng, W.W. Qu, Eur. Phys. J. A **49**, 10 (2013).
34. A.B. Balantekin, N. Takigawa, Rev. Mod. Phys. **70**, 77 (1998).
35. D. Vautherin, D.M. Brink, Phys. Rev. C **5**, 626 (1972).
36. G.R. Satchler, W.G. Love, Phys. Rep. **55**, 183 (1979).
37. D.T. Khoa, G.R. Satchler, Nucl. Phys. A **668**, 3 (2000).
38. W.D. Myers, W.J. Swiatecki, Nucl. Phys. **81**, 1 (1966).
39. W.D. Myers, W.J. Swiatecki, Ark. Fys. **36**, 343 (1967).
40. W.M. Seif, H. Mansour, Int. J. Mod. Phys. E **24**, 1550083 (2015).
41. D.T. Khoa, G.R. Satchler, W. von Oertzen, Phys. Rev. C **56**, 954 (1997).
42. D.N. Poenaru, W. Greiner, M. Ivascu, D. Mazilu, I.H. Plonski, Z. Phys. A **325**, 435 (1986).

43. G.L. Zhang, X.Y. Le, H.Q. Zhang, Nucl. Phys. A **823**, 16 (2009).
44. M. Ismail, A. Adel, Phys. Rev. C **86**, 014616 (2012).
45. H.F. Zhang, G. Royer, Y.J. Wang, J.M. Dong, W. Zuo, J.Q. Li, Phys. Rev. C **80**, 057301 (2009).
46. C. Xu, Z. Ren, Nucl. Phys. A **760**, 303 (2005).
47. N.S. Rajeswari, M. Balasubramaniam, J. Phys. G: Nucl. Part. Phys. **40**, 035104 (2013).
48. V. Zanganeh, N. Wang, Nucl. Phys. A **929**, 94 (2014).
49. M. Golshanian, O.N. Ghodsi, R. Gharaei, Mod. Phys. Lett. A **28**, 1350164 (2013).
50. R. Gharaei, V. Zanganeh, Nucl. Phys. A **952**, 28 (2016).
51. R. Gharaei, A. Hadikhani, Eur. Phys. J. A **53**, 147 (2017).
52. O.N. Ghodsi, R. Gharaei, Phys. Rev. C **88**, 054617 (2013).
53. N.S. Rajeswari, C. Nivetha, M. Balasubramaniam, Eur. Phys. J. A **54**, 156 (2018).
54. P. Moller, A.J. Sierk, T. Ichikawa, H. Sagawa, At. Data Nucl. Data Tables **109**, 1 (2016).
55. C.L. Guo, G.L. Zhang, X.Y. Le, Nucl. Phys. A **897**, 54 (2013).
56. P. Moller, J.R. Nix, Nucl. Phys. A **272**, 502 (1976).
57. H. Geiger, J.M. Nuttall, Philos. Mag. **22**, 613 (1911).
58. V.Yu. Denisov, H. Ikezoe, Phys. Rev. C **72**, 064613 (2005).
59. A. Bhagwat, Y.K. Gambhir, J. Phys. G: Nucl. Part. Phys. **35**, 065109 (2008).
60. V.Yu. Denisov, A.A. Khudenko, At. Data Nucl. Data Tables **95**, 815 (2009).
61. L.C. Vaz, J.M. Alexander, Z. Phys. A **318**, 231 (1984).
62. H. Vonach, R.C. Haight, G. Winkler, Phys. Rev. C **28**, 2278 (1983).
63. S. Gil, R. Vandenbosch, A.J. Lazzarini, D.K. Lock, A. Ray, Phys. Rev. C **31**, 1752 (1985).
64. A. Navin, V. Tripathi, Y. Blumenfeld *et al.*, Phys. Rev. C **70**, 44601 (2004).
65. C.S. Palshetkar, S. Santra, A Chatterjee, K. Ramachandran, Shital Thakur, S.K. Pandit, K. Mahata, A. Shrivastava, V.V. Parkar, V. Nanal, Phys. Rev. C **82**, 044608 (2010).
66. J.M. D'Auria, M.J. Fluss, L. Kowalski, J.M. Miller, Phys. Rev. **168**, 1224 (1968).
67. K.A. Eberhard, Ch. Appel, R. Bangert *et al.*, Phys. Rev. Lett. **43**, 107 (1979).
68. R. Broda, M. Ishihara, B. Herskind *et al.*, Nucl. Phys. A **248**, 356 (1975).